PPPL-2263

UC20-D,F,G

226
11/12/85 JS (2)

I-23795

(24)

PPPL-2263

PPPL--2263

DE86 002537

THREE NOVEL TOKAMAK PLASMA REGIMES IN TFTR

By

H.P. Furth

OCTOBER 1985

PLASMA PHYSICS LABORATORY

PRINCETON UNIVERSITY

PRINCETON, NEW JERSEY

PREPARED FOR THE U.S. DEPARTMENT OF ENERGY,
UNDER CONTRACT DE-AC02-76-CHO-3073.

THREE NOVEL TOKAMAK PLASMA REGIMES IN TFTR

Harold P. Furth

Princeton University, Plasma Physics Laboratory
Princeton, New Jersey 08544

ABSTRACT

Aside from extending "standard" ohmic and neutral beam heating studies to advanced plasma parameters, TFTR has encountered a number of special plasma regimes that have the potential to shed new light on the physics of tokamak confinement and the optimal design of future D-T facilities: (1) High-powered, neutral beam heating at low plasma densities can maintain a highly reactive hot-ion population (with quasi-steady-state beam fueling and current drive) in a tokamak configuration of modest bulk-plasma confinement requirements. (2) Plasma displacement away from limiter contact lends itself to clarification of the role of edge-plasma recycling and radiation cooling within the overall pattern of tokamak heat flow. (3) Noncentral auxiliary heating (with a "hollow" power-deposition profile) should serve to raise the central tokamak plasma temperature without deterioration of central region confinement, thus facilitating the study of alpha-heating effects in TFTR. The experimental results of regime (3) support the theory that tokamak profile consistency is related to resistive kink stability and that the global energy confinement time is determined by transport properties of the plasma edge region.

1. Introduction

During the past year, TFTR has reached its original machine design specifications (B_t = 5.2 T, I = 2.5 MA) and has begun the exploration of auxiliary heating regimes.[1,2] As illustrated in Fig. 1, a considerable range of plasma densities has already been explored in TFTR, thanks to the fairly strong toroidal field and the availability of an ORNL pellet injector.[3] The present state of progress towards fusion-relevant parameters is illustrated in Fig. 2, which follows a scheme suggested by J.G. Cordey: The central ion temperature is plotted vs. the central deuterium density times the "central region energy confinement time" (cf. Section 6). Initial neutral beam heating at powers up to 6 MW has been helpful in reaching high T_i in the low density plasma regime and high $n\tau_E$, along with moderately high T_i, in the high density regime.

A promising feature of the TFTR experiments has been that they have not only advanced the frontier of fusion plasma parameters, but have also uncovered some new physics that may turn out to be useful in guiding future tokamak research plans. The following three sections briefly discuss three TFTR regimes that have exhibited particularly interesting phenomena: low-density, hot-ion plasmas; adiabatically compressed plasmas in the free-expansion mode; and high density, noncentrally heated plasmas. Theoretical implications of the latter regime are pursued in Sections 5 and 6, and prospects for the TFTR D-T phase are summarized in Section 7.

2. The Energetic Ion Regime

In the TFTR energetic ion regime, the central electron density typically rises from $1.5 \cdot 10^{13}$ cm^{-3} to $3 \cdot 10^{13}$ cm^{-3} during the injection of beam particles. The central electron temperature T_{eo} is 3-4 keV. The energetic ion component, which is characterized by a mean slowing-down energy of 35-45 keV, constitutes an estimated 2/3 of the central ion density. An appropriately low level of background plasma density so as to permit entry into this regime can be obtained in TFTR by operating at reduced plasma currents (typically 800 kA). The total energy confinement time is then found to be of order 70 msec, with the plasma energy stored mainly in the ions. The average central region ion energy, including all components, is in the range 20-40 keV. The well-thermalized "cold background ions" have a central temperature close to 10 keV.

The TFTR energetic ion regime exhibits some remarkable incidental phenomena. The toroidal rotation velocity rises to ~6 • 10^7 cm/sec, corresponding to a rotational kinetic energy ~4 keV for deuterons and ~100 keV for heavy impurity ions. (The momentum confinement time is found to be of the same order as τ_E.) There is also strong evidence that the injected ions are driving an appreciable part of the plasma current, in agreement with theoretical expectation. The intensive beam fueling apparently serves to depress Z_{eff} from its average value of 4-5 to a level of $\lesssim$2 near the axis.

The success of the initial TFTR experiments in the energetic ion regime offers some encouraging prospects. As the beam power is raised from 6 MW to its nominal value of 27 MW (with the full-energy component rising from 3 MW to 20 MW) the energetic ion regime should be maintainable up to somewhat higher plasma densities, thus permitting higher current operation, greater $n\tau_E$-values for the background plasma, higher T_e, and correspondingly slower thermalization rates for the hot ions.

The expected fusion yields in the TFTR energetic ion regime were calculated for deuterium plasma by means of a Fokker-Planck code[4] that has given accurate predictions in the case of previous neutral beam injection experiments, such as PLT.[5] At present, the calculated TFTR neutron yields tend to exceed the measurements by a factor of about 1.5-2.0. (The larger discrepancy is found systematically at higher density, but its origin has not yet been identified.) Figures 3a and 3b illustrate the predictions of the code of Ref. 4, respectively, for the low density regime ($n_{eo} \lesssim 6 \cdot 10^{13}$ cm^{-3}), where essentially all the central region ions are energetic, and for a moderate density regime ($n_{eo} \lesssim 10^{14}$ cm^{-3}), where the energetic ion component typically accounts for only a small fraction of the central ion population. The object of these studies was to compare the Q-values and dominant reaction processes of low and moderate density TFTR regimes characterized by the same central electron temperature [T_{eo} = 10 keV (P/15 MW)$^{1/2}$]. The calculations of Fig. 3 assumed balanced co- and counter-injection at 120 keV and used a realistic beam-species mix. The code takes the actual orbits of the energetic ions into account; ions are removed from the energetic population when they have decelerated to an energy of (3/2) T_i. The calculations were time stepped until steady-state conditions were reached.

Figure 3a shows that beam-beam reactions strongly predominate in low density TFTR deuterium plasmas. If balanced D and T injection were used, the $Q_{DT} = 1$ point would ideally be achievable with 13 MW of input power. (This result is, of course, contingent on attainment of the specified T_{eo} and Z_{eff}; if, for example, the central region Z_{eff} were 2.5 rather than ~1.0, then 25 MW of beam would be required to reach $Q = 1$.) In the moderate density deuterium case of Fig. 3b, two-component (TCT) reactions tend to dominate, but the contribution of ordinary thermonuclear reactions is also important. For an idealized D-T case where a 100% tritium target plasma is used so that only TCT reactions occur, the $Q = 1$ point is reached at 22 MW. (Since thermonuclear and beam-beam reactions are seen to account for about half of the total D-D fusion yield, the case with balanced D and T injection gives a similar result: i.e., the Q-value is not very sensitive to the species mix.)

The tentative conclusion of these studies is that the low density regime may well offer a path of least resistance to the achievement of $Q = 1$. For example, the ideal $n(o)\,\tau_{Ee}$-value for the electrons could be as small as $\sim 3 \cdot 10^{12}$ cm^{-3} sec in the low density case, as compared with $\sim 5 \cdot 10^{12}$ cm^{-3} sec in the moderate density case.

Turning to the potential for practical application of the energetic ion regime, the possibility of achieving Q-values in the range $\gtrsim 1$ by means of counter-injected deuterium and tritium beams was pointed out in Ref. 6 as an interesting approach to a moderate-sized tokamak test reactor. The initial TFTR observations indicate that the required combination of good energetic ion confinement and rapid removal of the thermalized ion component may be achievable in practice. A critical issue will be, whether the beam-fueling process will indeed "flush out" the impurity ions, so that Z_{eff} can be kept small. The TFTR results tend to confirm that a true steady-state tokamak plasma regime could be maintained by biasing the injected momentum so as to provide beam current drive. Some representative parameters for a tokamak radiation test facility based on this concept might be: $R = 3$ m, $I = 2.5$ MA, beam power ~ fusion power ~ 100 MW, neutron wall loading $0.5 - 1.0$ MW/m^2.

3. Adiabatic Compression and Free Expansion

In a gross sense, the major-radius compression technique works well in TFTR: the plasma temperature and density increase,[7] the energy of beam-injected ions is doubled,[8] and fusion reaction rates are enhanced correspondingly. Adiabatic compression heating is, in principle, the least intrusive and most predictable of auxiliary heating methods. In practice, however, the initial TFTR experiments have demonstrated an anomalous loss of plasma density and energy content during compression (cf. Fig. 4) that corresponds to a noticeable degradation of confinement relative to the precompression state.

One potential defect of the initial TFTR compression experiments has been found to relate to resistive MHD instability[9] (cf. Fig. 5). During the first phase of the compression, while the plasma major radius R is moving to the center of the vessel ($R_o \sim 2.5$ m), the q-value at the vessel wall is rising continuously (Fig. 5a). The subsequent forced decrease of this q-value is seen to be accompanied by a sequence of MHD kink oscillations (Fig. 5b) much like those usually found during the initial TFTR current rise. The apparent cause of this phenomenon is the induction and unstable relaxation of skin currents in the supposed "vacuum region" between the compressed plasma core and the vessel wall -- which in fact turns out to be a region of quite good electrical conductivity. Since the appearance of the magnetic oscillations is found to coincide in time with various anomalies on the interior of the hot plasma, the skin-relaxation phenomenon could turn out to be at least partly responsible for the nonadiabaticity of the TFTR compression.

In addition, however, there must clearly be a more fundamental problem: When the plasma is compressed only to the midway point so that the low-frequency oscillations of Fig. 5 are not encountered, one still observes the high-frequency component of the magnetic probe signal, as well as an anomalously rapid broadening of the temperature and density profiles. During this "free expansion phase," where the edge of the hot-plasma core is remote from the usual tokamak limiter contact, the plasma is not exposed to the usual cooling by influx of impurities and recycling hydrogen gas. The normal relationship between the $T_e(r)$ and $n(r)$ profiles is then interchanged, with the $T_e(r)$-profile becoming the broader of the two. The

paradoxical result for energy confinement is that removal of the normal edge-cooling processes seems actually to enhance the rate of heat transport (which can be inferred from the rate of profile broadening, even though the total energy content of the free-expansion plasma tends to be conserved). There is a possible explanation in terms of microinstability phenomena excited at the plasma edge when the local value of d(log n)/d(log T) or $J/nT^{1/2} \propto T/n$ becomes too large. The free-expansion plasma appears to offer yet another among a growing list of examples where tokamak transport throughout the plasma volume is enhanced by changes in edge-plasma conditions. This topic is pursued at greater length in Section 6.

4. Noncentral Heating

If tokamak heat transport were describable in terms of a simple local diffusivity $\chi(r)$, then energy confinement would be maximized by depositing all heating power at $r = 0$. The inadequacy of this type of confinement model was shown clearly by the T-10 ECRH studies[10]: the gross energy confinement time τ_E was found to remain roughly constant during a shift of the resonance point from $r = 0$ out to $r/a \sim 0.7$. That this phenomenon is not peculiar to the ECRH regime was subsequently shown in TFTR[11] by comparing two neutral beam injection cases with the same target plasma, beam-particle energy, and input power: a hydrogen beam case with a centrally peaked beam-power deposition profile $P_H(r)$, and a deuterium beam case with "hollow" $P_H(r)$. The τ_E-values for these two cases were found to be nearly identical -- as were the $T_e(r)$ profiles and peak temperatures T_{eo}. Similar results have been found for neutral beam heating in ASDEX.[12]

TFTR experiments where reduced beam penetration is achieved by combining pellet densification with neutral beam injection[13] (cf. Fig. 6a), have demonstrated the same phenomenon in even more striking form: While the peak of $P_H(r)$ lies at $r/a \sim 0.8$, the associated $T_e(r)$ profile (Fig. 6b) closely resembles that of the hydrogen beam case of Ref. 11, and the measured values of τ_E and T_{eo} are found to remain consistent with the normal empirical scaling laws for neutral beam heating.

The observed insensitivity of gross confinement to the heating-power deposition profile implies that central region confinement must become very favorable as $P_H(r)$ is made increasingly hollow. Using the steady-state definition

$$\tau_E(r) = \frac{3/2\int_o^r dr_1\ r_1\ n(T_e + T_i)}{\int_o^r dr_1\ r_1\ P_H(r_1)} \qquad (1)$$

with the total imput power corrected for $dn(T_e + T_i)/dt$, to obtain P_H, the authors of Ref. 13 find that in the case of Fig. 6 very high values of $\tau_E(r)/\tau_E(a)$ are indeed reached for $r/a \sim 0.5$, where $\tau_E(a)$ is the conventional definition of τ_E. This finding is reflected in the favorable position of the "NB Pellet" data points in Fig. 2.

One notes, incidentally, that large interior values of $\tau_E(r)$ could be obtained trivially for T(r)-profiles that are <u>flat</u> over the region of interest, but since the actual temperature profile remains peaked in Fig. 6b, the $\tau_E(r)$-variation in Fig. 6c must reflect a genuine reduction in the central region values of $\chi(r)$. In contrast to the phenomenon of Fig. 6b, one finds in stellarators with noncentral ECRH that the $T_e(r)$-profile behaves in the normally expected way, becoming quite flat on the interior of the region of peak power deposition.[14]

5. Tokamak Profile Consistency and Resistive Kink Stability

A certain family resemblance of tokamak $T_e(r)$-profiles has long been noted in the experiments. The potential importance of this phenomenon for the theory of anomalous tokamak transport was pointed out by B. Coppi[15] and has also been pursued by F.W. Perkins[16] and others. These analyses have made use of the obvious constraints on the current-density profile J(r) that result from the two boundary conditions on the MHD safety-factor profile: $q(0) \gtrsim 1$ and $q(a) = B_t a^2/2IR$. If one makes an <u>ad hoc</u> selection of a specific current-profile shape -- such as the Gaussian -- these constraints are sufficient to define the magnitude and shape of J(r) uniquely, and therefore also to define the shape $T_e(r)/T_{eo}$ (but not the magnitude of T_e) in resistive steady state.

Detailed studies of resistive kink mode stability[17-19] suggest that an <u>ad hoc</u> profile-shape assumption may not be necessary: For specified q(o)- and q(a)-values, the requirement of kink stability (negative Δ') at all mode numbers m and n imposes fairly narrow constraints on the J(r)-profile, even when q(a) is large; as q(a) is reduced, the J(r)-profile is channeled into singular shapes; finally, when the q(a)-value has approached too close to

the important 2/1 resonance, there is no solution at all. [These remarks assume the ordinary experimental case. If there is an effective external stabilizing shell or plasma layer, and/or if the time-averaged q(o)-value is permitted to go below unity,[19] then kink-stable J(r)-profiles may be maintainable all the way down to the vicinity of the 3/2 resonance.]

Do actual tokamaks follow the prescriptions of Δ'-stability analysis? Current TFTR studies,[20] based on detailed radial T_e-measurements and computations of J(r) by means of the TRANSP Code, indicate that the TFTR plasma is fairly adept at Δ'-minimization. For $q(a) \gtrsim 4$, the experimentally derived Δ's are generally either negative at all m and n, or are positive, but sufficiently small so that the corresponding magnetic islands are calculated to remain narrow and localized. In the range $q(a) \lesssim 3$, where the maintenance of an all-negative set of Δ's is a more difficult problem, the calculations show that islands of moderate size tend to be present continuously. Actual disruptions are found to occur experimentally at times when the computed Δ's show a strong increase, corresponding to an excursion of J(r) from near-optimality. On the whole, Ref. 20 offers considerable support for the predictions of Δ' analysis, but the available results are still preliminary; in particular, the computation of the experimental J(o) is subject to the usual uncertainties of how best to model the combination of neoclassical resistivity and sawtooth activity. Figure 7 gives a (slightly idealized) illustration of the range of stable J(r)-profiles in TFTR: (A) The high-q(a) case is generally seen towards the end of the current-ramp-up phase; (B) the low-q(a) case is typical of steady-state operation.

How might the tokamak plasma manage to find minimum-Δ' solutions? One possibility would be that a modified form of Taylor's "dynamo mechanism" is at work, as in the RFP. In view of the paucity of unstable modes, however, this seems unlikely, and one is led instead to a model where heat transport is enhanced in the vicinity of those singular points $q(r_{mn}) = m/n$, where $\Delta' \gtrsim 0$. Particularly if this phenomenon occurs mainly towards the small-r side of the singular points, the resultant local flattening of $T_e(r)$, and therefore of J(r), tends to stabilize the m/n kink by reducing dq/dr at r_{mn} -- while, of course, impairing the stability of modes with neighboring values of m/n by steepening the q(r)-profile at their singular points.[17]

This type of self-adjustment would seem fairly effective as a computer scheme[21] for finding minimum-Δ' profiles. There is no direct experimental evidence, however, that it occurs in tokamaks: Substantial magnetic oscillations are seen only just prior to disruptions; stationary magnetic islands could go undetected by magnetic probes -- and might be considered a logical consequence of magnetic coupling to imperfectly conducting external stabilizing shells or plasma layers -- though the maintenance of their invisibility in rotating plasmas may present special problems.

There are still other possibilities: An important one is that the condition $\Delta' \gtrsim 0$ may encourage the formation of electrostatic convective cells near the singular points. Even MHD-unrelated transport phenomena, such as microinstabilities, could give rise fortuitously to resistive kink stable profiles. (The plausibility of this suggestion is enhanced if we consider that tokamak experimentalists are part of the feedback loop: They adjust the operating parameters and "condition" the tokamak vacuum chamber until stable profiles are achieved; then they take "real tokamak data.") Fortunately, the discussion of tokamak energy confinement in the next section does not depend on the nature of the profile-selection process -- only on the assumption that experimental $J(r)$-profiles must tend naturally towards Δ'-stability.

6. Energy Confinement in the Tokamak

The principle of profile consistency[15] may help account for a number of apparent tokamak anomalies. The Alcator C group[22] found a surprisingly rapid restoration of the standard $T_e(r)$-profile following injection of a pellet partway into the tokamak plasma. Coppi has suggested that gross resistive instabilities may be responsible, and that the physical mechanism is similar to that causing enhanced outward propagation of heat pulses originating from the sawtooth mechanism. In both cases, the allusion to resistive kink mode theory requires that very small perturbations of $J(r)$, arising from perturbations in $T_e(r)$ on a resistive-diffusion time scale, should have a relatively drastic impact on local transport.

Strong supporting evidence for tokamak profile consistency is provided by noncentral tokamak heating experiments, such as that of Fig. 6. These results also support a fairly persuasive argument that the profile of $J(r)$, rather than of $T_e(r)$, is the key issue: The conspicuous absence of the

profile-consistency phenomenon in edge-heated stellarators[14] implies that the need to provide resistive kink stability may indeed be responsible for the tokamak profile shape.

The assumption of profile consistency can be used to deduce from the data of Fig. 6 yet another interesting aspect of tokamak confinement: The "global confinement time" τ_E must reflect the magnitude and scaling of the local transport coefficient $\chi(r_c)$ at some radius fairly close to the plasma edge (typically $r_c/a \gtrsim 0.7$). For the sake of simple illustration, the following analysis will neglect convection and ion heat conduction (assuming $T_e = T_i = T$) and will identify profile consistency with Δ'-stability. The heat flow equation is written as

$$-n(r)\,\chi(r)\,\frac{dT}{dr} = \phi(r) = \frac{1}{r}\int_0^r dr_1\, r_1\,(P_H - P_R), \tag{2}$$

where P_R is the radiation cooling power. If a profile shape is prescribed according to $T = T_s(r) = T_o F_s(r/a)$, then $\chi(r)$ follows from

$$\chi(r) = \frac{-\phi(r)\,a}{n(r)\,T_o\,F'(r/a)}, \tag{3}$$

where $\phi(r)$ and $n(r)$ can be viewed as controllable by the experimenter, while $\chi(r)$ and T_o are experimental results. We see at once that, if T_o remains constant while $\phi(r)$ is varied, $\chi(r)$ can be made arbitrarily small -- and correspondingly $\tau_E(r)$ can be made arbitrarily large in the central plasma region -- by choosing a pattern of noncentral heat deposition, as in Fig. 6.

What determines the central temperature T_o? According to Eq. (3), T_o is quite arbitrary too, but in reality there must be some lower bound on $\chi(r)$, imposed by an "irreducible" heat transport rate $\chi_m(r)$, which includes neoclassical diffusion at a minimum, and may contain strong anomalous enhancements as well. Rewriting Eq. (2) in the form

$$-n(r)\left\{\chi_m(r) + \chi_s(r)\right\}\frac{dT}{dr} = \phi(r), \tag{4}$$

we define $\chi_s(r)$ as the transport enhancement needed to give the desirable temperature profile. In general, there is some degree of latitude in the Δ' stability condition, so that $T/T_o = F_s(r/a)$ need not be enforced precisely at all radii. Accordingly, we can think in terms of two different types of transport region: In Region I, the profile $F_s(r/a)$ is maintained by appropriate variations of $\chi_s(r)$. In Region II, the local value of $\chi_m(r)$ is such that $\chi_s(r)$ would have to become negative to maintain F_s. Since the best we can actually do is $\chi_s = 0$, it follows that in Region II the T(r)-profile is determined in the "normal" way by χ_m alone:

$$-n(r)\,\chi_m(r)\,\frac{dT_m}{dr} = \phi(r). \tag{5}$$

In this region, we write $T = T_m(r)$, which generally will not coincide with $T_s(r)$. The vanishing of χ_s at the interface ensures that regions of types I and II are tied together by a T(r)-profile with continuous T and dT/dr. Since χ_m is a real physical transport coefficient, it determines the magnitude of dT_m/dr, and therefore of the whole T(r)-profile, when $\phi(r)$ and n(r) are specified.

The noncentral heating experiments are a powerful tool for discovering in what ranges of the tokamak profile type-II regions are located. Equation (5) implies that there will be a clear difference in the magnitude of the local dT/dr, depending on whether $P_H(r)$ is peaked inside or outside a type-II region, since the associated heat flux ϕ through the region will be correspondingly different. The tokamak experiments exhibit relatively little overall temperature variation or profile change for $P_H(r)$ peaked at various radii out to $r/a \gtrsim 0.7$, thus demonstrating that type-II regions can only lie at the outer edge of the tokamak profile. This conclusion is consistent with the experimental observation that changes in edge-plasma conditions (such as neutral hydrogen influx or impurity admixture) affect transport rates throughout the tokamak plasma. For simplicity we will assume a single Region II, extending to the limiter; however, in the case of tokamak plasmas bounded by a separatrix -- for which the Δ'-analysis would tend to yield appreciably different requirements -- there may well be a (bistable?) type-I profile at the very edge of the plasma.

We now consider more detailed implications of the Δ'-interpretation of profile consistency for the overall structure of the tokamak temperature profile. Experimentally, one finds that both χ_m and P_R increase towards the plasma edge, so that temperature profiles in Region II tend to have positive curvature. The T_s-curve shown in Fig. 8, on the other hand, reflects the critical importance of maintaining a limited downslope of temperature at the $q = 2$ point. The presence of a T_m-type profile at $q = 2$ would be expected to result in $m = 2$, $n = 1$ instability -- a prediction that is readily verified in tokamak experiments with enhanced edge-radiation cooling. If instability is to be forestalled by the benign action of a profile-shaping diffusivity χ_s, then clearly r_c should lie outside the $q = 2$ point.

It is also easy to see that r_c will tend to move towards the smallest permissible radius. The plasma heating process in Region I tends to push the temperature up against the stability limit $T_s(r)$, which in turn must always lie below the extrapolated T_m-curve. (This is because χ_s can only act to diminish confinement -- i.e., the plasma would be hotter in the absence of MHD activity.) The least restrictive temperature limitation is obtained when T_s and T_m coincide to the maximum permissible extent -- i.e., when r_c is as small as possible. With a bow to the authors of Ref. 10, one concludes that the most natural location for r_c is just outside the $q = 2$ point. If this conclusion is correct, it follows that in the case of Fig. 6 the global τ_E could be improved somewhat by shifting the power deposition to smaller radii.

The present line of argument also allows us to clear up an apparent weakness of the Δ'-version of profile consistency: namely, that even for fixed $q(o)$ and $q(a)$ the set of permissible $J(r)$-profiles generally has some finite breadth -- whereas a physically meaningful profile-consistency model should offer a truly singular prescription for $T_s(r)$. The apparent latitude in $T(r)$ can be eliminated by the auxiliary hypothesis that the plasma temperature will "push up" towards its highest Δ'-stable, or nearly Δ'-stable profile. (A conspicuous illustration of this process is provided by tokamak plasmas at the $q > 1$ stability boundary.) A specific $T_s(r)$-profile selected in this way seems likely to show at least some dependence on the distribution of $P_H(r)$ -- as appears to be the actual case in the experiments. Another side benefit of this model is that, if the steady-state

temperature profile is assumed to be pressing against the very edge of the family of Δ'-stable curves, then a fast response to heat-pulse propagation or pellet injection becomes easier to understand.

The Δ'-model of profile consistency provides a natural explanation of the evolution of the electron temperature profile during the tokamak current-rise phase. Initially, a skin current tends to form, giving highly Δ'-unstable nonmonotonic J(r)-profiles, which relax rapidly. Subsequently, a centrally peaked profile, like that of Fig. 7, Type A, can maintain itself stably as long as q(a) is still fairly large. The final phase is characterized by sawtooth activity in the $q < 1$ region, with the Type-B profile emerging as q(a) decreases to its steady-state value. The present argument that the magnitude of T_{eo} is determined by dT_e/dr near the plasma edge, tends to account naturally for the experimental observation that the highest values of T_{eo} occur transiently for the centrally peaked Type-A profiles, while a somewhat higher total energy content is measured subsequently during the Type-B steady-state phase.

What are the implications for global tokamak energy confinement? According to the present picture, the heating power P_H should be concentrated inside r_c so that its contribution to the heat flux ϕ may help raise $|dT/dr|$ at the critical point r_c where the magnitude of the temperature profile is determined. For the same reason, one desires to minimize the radiation cooling power P_R in the region inside r_c. Assuming, for simplicity, that P_H vanishes in the region $r > r_c$ while P_R vanishes for $r < r_c$, we conclude from Eqs. (1) and (2)

$$\tau_E(a) \gtrsim \tau_E(r_c) \propto \frac{\langle n \rangle T_o a}{\phi(r_c)} \propto \frac{\langle n \rangle a^2}{n(r_c)\,\chi(r_c)}, \tag{6}$$

where an average density $\langle n \rangle = (2/a^2) \int_0^r dr_1\, r_1\, n(r_1)\, F_s(r_1/a)$ has been defined. Equation (6) has several interesting implications:

1. "Empirical" scaling laws for τ_E do not tell us anything about the physics of microscopic transport in the hot, central part of the tokamak plasma.

2. The exact nature of the plasma heating power input in the region $r < r_c$ is unlikely to have a direct effect on τ_E (though side effects of auxiliary heating at the plasma edge may be important).

3. The "degradation" observed with strong auxiliary heating must be due mainly to associated changes in local plasma parameters at r_c. In the case of the empirical scaling of Ref. 23, this point of view would suggest $\chi_m(r_c) \propto d\beta_p/dr$ -- but one can also interpret the Ref. 23 scaling in terms of $\chi_m(r_c) \propto \phi^{1/2}(r_c)/B_p$.

4. *Central peaking of the density profile is helpful for enhancing* τ_E, as illustrated by the "OH Pellet" points in Fig. 2 [but large values of $d(\log n)/d(\log T)$ or $J/nT^{1/2} \propto T/n$ near the plasma edge may well be damaging to $\chi(r_c)$, as suggested by the TFTR free-expansion experiments of Section 3].

5. *If an MHD-related profile-shaping mechanism is depressing tokamak temperatures,* the "irreducible" central region confinement properties may yet turn out to be quite favorable. Suppression of the $m = 1$ mode should clearly be advantageous.[19] Another promising approach will be to establish better control over the edge plasma, which at present is relatively poorly confined and therefore potentially suitable -- as well as conveniently accessible -- for improvement by special techniques. In this connection, the L-mode/H-mode transition comes to mind. Extension of the Δ'-analysis to noncircular geometry might help us to understand the nature of this phenomenon and perhaps stimulate further improvements of tokamak edge confinement.

7. Initial D-T Experiments

Current experimental developments on TFTR suggest that the exploration of two special D-T plasma regimes may prove to be particularly rewarding: (1) The low density, energetic ion regime is expected to facilitate the achievement of $Q = 1$, and could be of substantial nuclear engineering interest as the prototype of a compact steady-state fusion test reactor. (2) The high density, noncentrally heated regime should lend itself particularly well to the detection and study of alpha-heating effects, since the central plasma region is expected to have relatively favorable $n\tau_E$-values, along with minimal levels of nonfusion background power deposition. An

experiment of particular interest will be to create a moderate-$q(a)$ deuterium plasma regime with weak sawtooth activity and look for α-driven sawtooth excursions when tritium fuel is added.

The combination of these two types of experiments in the TFTR D-T phase seems likely to make a useful contribution to both the physics of burning plasmas and the engineering of fusion reactors.

Acknowledgments

I should like to thank Drs. E. Fredrickson, A.H. Glasser, D.L. Jassby, K.M. McGuire, and P.H. Rutherford for valuable discussions of their results.

Work supported by DoE Contract No. DE-AC02-76CH03073.

References

/1/ TFTR GROUP (presented by R.J. Goldston), Workshop on Basic Physical Processes of Toroidal Fusion Plasmas (Varenna, Italy), August 26-31, 1985 (to be presented).

/2/ MURAKAMI, M., et al., Proc. 12th European Conf. on Cont. Fusion and Plasma Physics (Budapest, Hungary), September 2-6, 1985 (to be presented).

/3/ COMBS, S.K., MILORA, S.L., FAUST, C.R., FOSTER, C.A., and SCHERESKI, B.D., Rev. of Sci. Instrum. 56 (1985) 1173.

/4/ MIRIN, A.A. and JASSBY, D.L., IEEE Trans. Plasma Sci. PS-8 (1980) 503.

/5/ MIRIN, A.A., et al., Proc. Joint Varenna-Grenoble Inst. Symposium on Heating in Toroidal Plasmas, Ed. T. Consoli (Pergamon, Oxford, 1979) Vol. I, 13.

/6/ KULSRUD, R.M. and JASSBY, D.L., Nature (London) 259 (1976) 541.

/7/ WONG, K.L., et al., submitted to Phys. Rev. Lett.

/8/ TAIT, G.T., et al., Proc. 10th Internat. Conf. on Plasma Physics and Controlled Nuclear Fusion Research, London, 1984 (IAEA, Vienna, 1985) Vol. 1, 141.

/9/ GREK, B., JOHNSON, D., BOODY, F., KIRALY, J., MCGUIRE, K., PARK, H., TAIT, G., TAYLOR, G., WONG, K.L., and STAUFFER, F., Proc. 27th American Physical Society Division of Plasma Physics Meeting (San Diego, California), November 4-8, 1985 (to be presented).

/10/ ALIKAEV, V.V., et al., Plasma Phys. and Cont. Nucl. Fusion Research I (1984) 419.

/11/ MURAKAMI, M., et al., Princeton Plasma Physics Laboratory Report No. PPPL-2224 (June 1985); Proc. 6th Topical Meeting on the Technology of Fusion Energy (San Francisco, California), March, 1985.

/12/ KEILHACKER, M., private communication.

/13/ SCHMIDT, G.L., et al., Proc. 12th European Conf. on Cont. Fusion and Plasma Physics (Budapest, Hungary), September 2-6, 1985 (to be presented).

/14/ GRIEGER, G., private communication.

/15/ COPPI, B., Comments Plasma Phys. Cont. Fusion 5 (1980) 261.

/16/ TANG, W.M., et al., Plasma Phys. and Cont. Nucl. Fusion Research II (1984) 213.

/17/ FURTH, H.P., RUTHERFORD, P.H., and SELBERG, H., Phys. Fluids 16 (1973) 1054.

/18/ GLASSER, A.H., FURTH, H.P., and RUTHERFORD, P.H., Phys. Rev. Lett. 38 (1977) 234.

/19/ RUTHERFORD, P.H., HSUAN, H., and IGNAT, D., Workshop on Basic Physical Processes of Toroidal Fusion Plasmas (Varenna, Italy), August 26-31, 1985 (to be presented). FURTH, H.P., et al., Proc. 12th European Conf. on Cont. Fusion and Plasma Physics (Budapest, Hungary), September 2-6, 1985 (to be presented).

/20/ FREDRICKSON, E., CALLEN, J., COLCHIN, R.J., MCGUIRE, K., PARE, V., SAUTHOFF, N., and ZARNSTORFF, M.C., Proc. 27th American Physical Society Division of Plasma Physics Meeting (San Diego, California), November 4-8, 1985 (to be presented).

/21/ TURNER, M.F. and WESSON, J.A., Nucl. Fusion 22 (1982) 1069.

/22/ GREENWALD, M., et al., Proc. 10th Internat. Conf. on Plasma Physics and Controlled Nuclear Fusion Research, London, 1984 (IAEA, Vienna, 1985) Vol. 1, 45.

/23/ GOLDSTON, R.J., Plasma Physics and Cont. Fusion 26, 1A (1984) 37.

Figure Captions

Fig. 1. Plasma density range of the initial TFTR experiments. Strong central peaking is obtained during low density ohmic and neutral beam heating and high density pellet injection.

Fig. 2. The TFTR "Cordey diagram." Central ion temperatures are plotted against the product of deuterium ion density and central-region energy confinement time in the central region.

Fig. 3. Q-values are calculated[4] for (a) low density and (b) moderate density TFTR deuterium plasmas at various neutral beam injection powers. The relative importance of the individual fusion-reaction mechanisms is also shown. The minimum power requirement for D-T breakeven is indicated by the dashed line.

Fig. 4. Degradation of energy confinement during adiabatic compression[7] is implied by the marked divergence of measured electron temperature profiles (dashed lines) from the ideal adiabatic predictions (solid lines).

Fig. 5. During major-radius compression, the q-value at the surface of the plasma core remains constant, but the q-value at the vacuum chamber wall (a) must first increase and then return to its starting value. The declining phase of q is accompanied by MHD oscillations (b): the last three bursts have been identified[9] as m/n = 6/1, 5/1, and 4/1 kinks. The associated R-variation is shown in (c).

Fig. 6. Neutral beam injection (5 MW D) into a plasma of 10^{14} cm^{-3} central density (I = 2.2 MA, B_t = 4.8 T) gives rise to the noncentral power-deposition profile (a). The electron temperature profile, however, remains normal (b), as does the global energy confinement time τ_E. When computed as a function of r, τ_E is found to be strongly enhanced in the central plasma region.

Fig. 7. Two tokamak current-density profiles having positive Δ'-stability except in the $q < 1$ region, which were selected for their resemblance to typical TFTR cases[20]: (A) $q(o) = 1$ and a large $q(a)$-value (~ 5); (B) $q(o) \lesssim 1$, and a reduced $q(a)$-value (~ 2.8).

Fig. 8. Qualitative picture of the transition from Region I to Region II. The edge-plasma temperature profile T_m is matched to the MHD-stable profile T_s at r_c. Profiles of the form T_m^R, resulting from excessive edge radiation cooling, tend to be incompatible with the preservation of kink stability at $q = 2$.

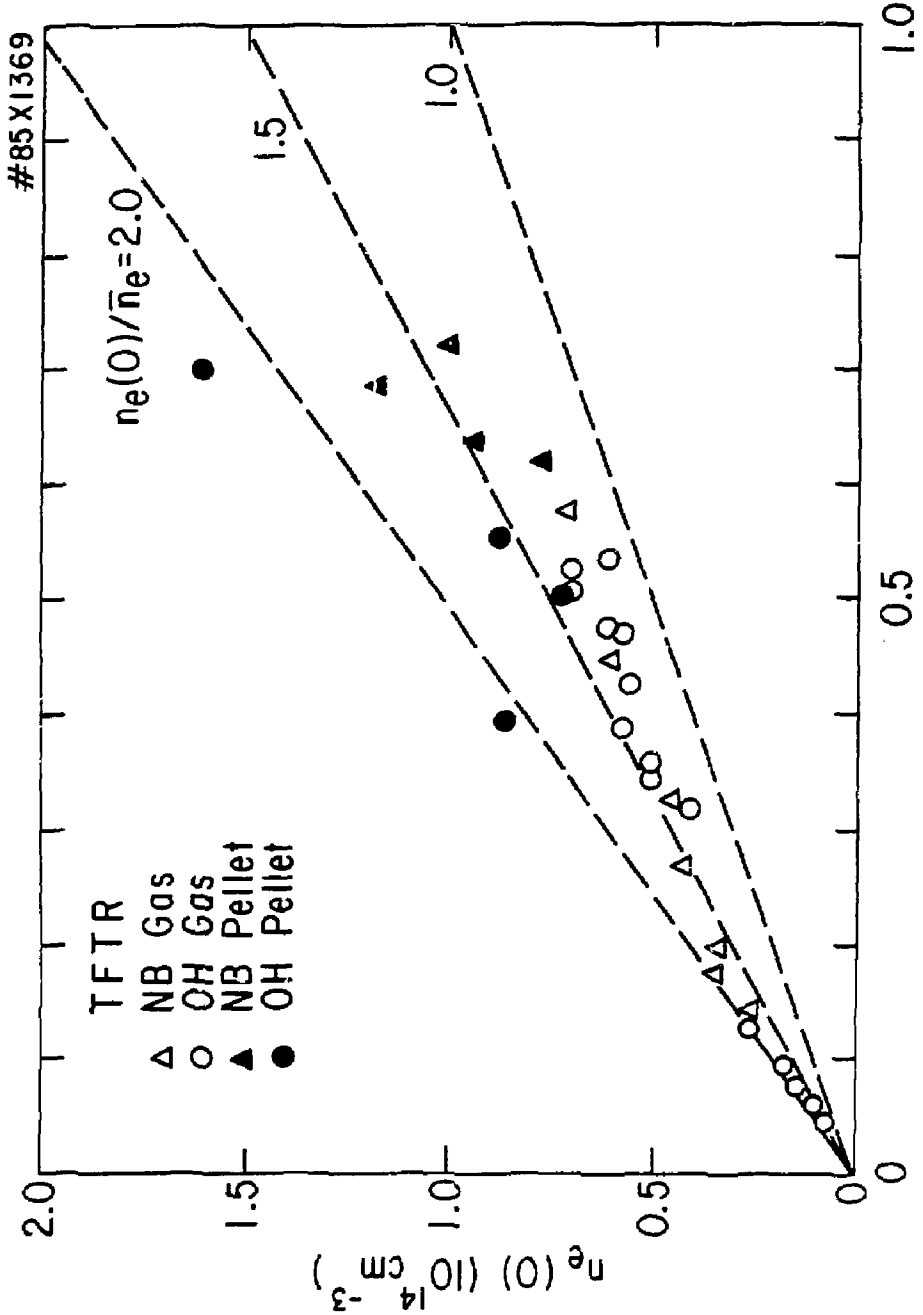
#85X1369
$n_e(0)/\bar{n}_e=2.0$
1.5
1.0
TFTR
NB Gas
OH Gas
NB Pellet
OH Pellet
$n_e(0)$ (10^{14} cm^{-3})
$\bar{n}_e$ (10^{14} cm^{-3})
0
0.5
1.0
1.5
2.0

Figure 1

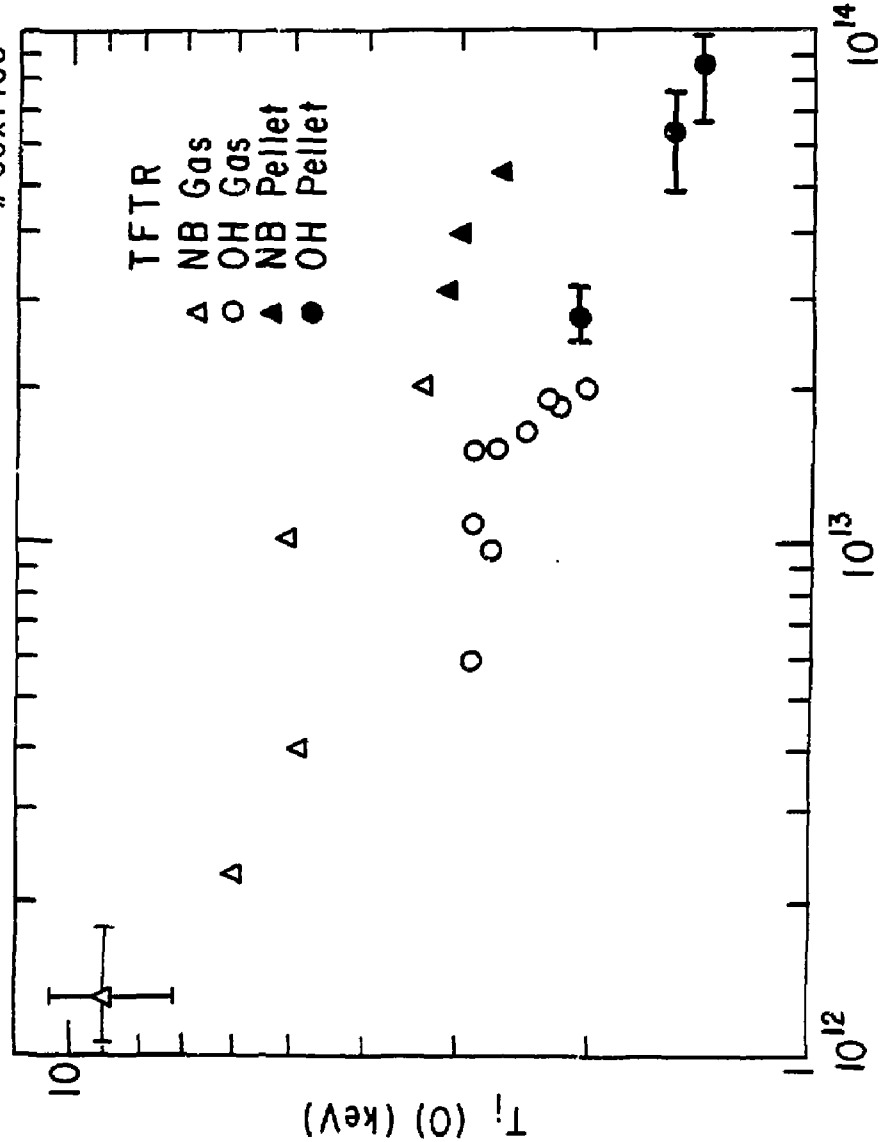
#85X1408
TFTR
NB Gas
OH Gas
NB Pellet
OH Pellet
T_i (0) (keV)
10
1
10^{12}
10^{13}
10^{14}
$n_D(0)\,\tau_E\,(a/2)\,cm^{-3}sec$

Figure 2

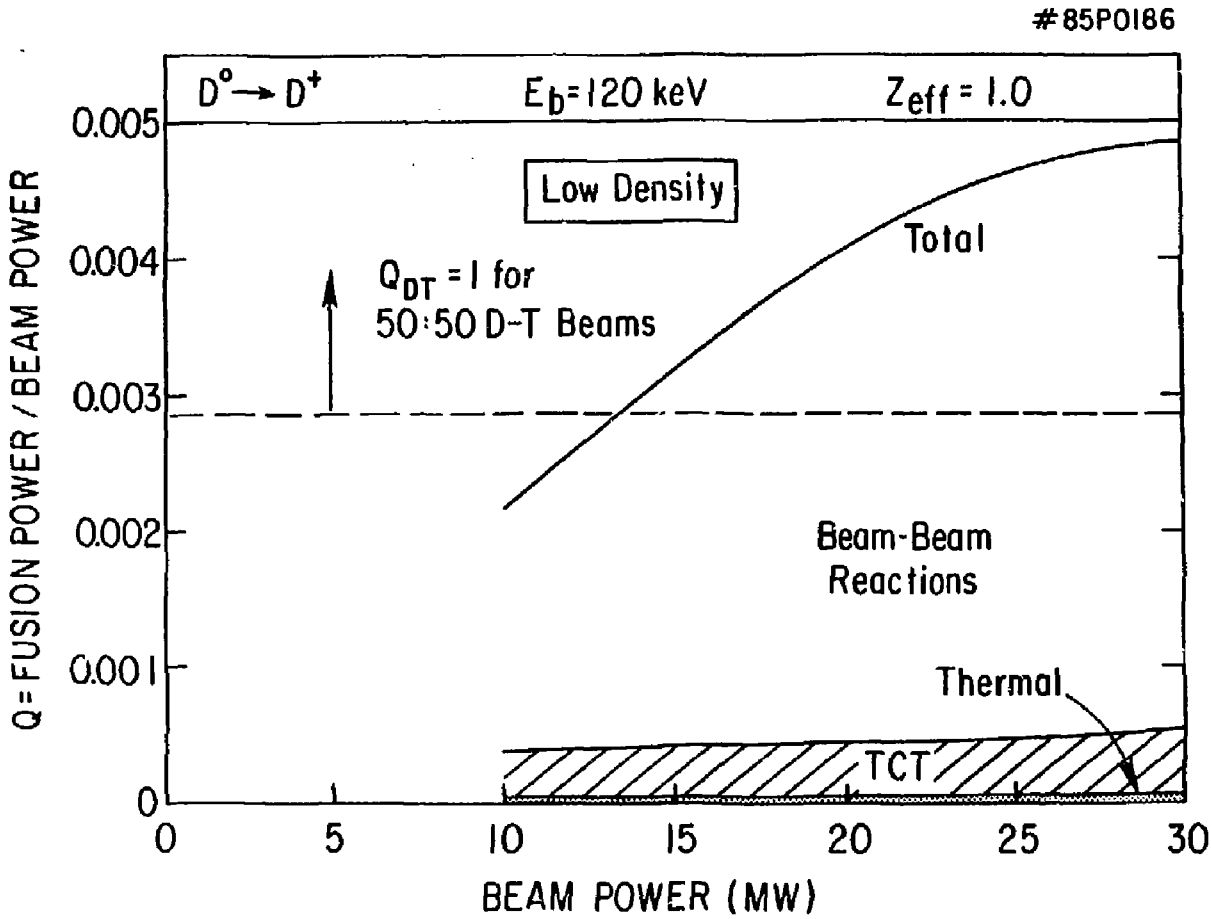
#85P0186
D°→ D⁺
Eb=120 keV
Zeff = 1.0
Low Density
Total
QDT = 1 for
50:50 D-T Beams
Beam-Beam
Reactions
Thermal
TCT
Q = FUSION POWER / BEAM POWER
BEAM POWER (MW)
0.005
0.004
0.003
0.002
0.001
0
0
5
10
15
20
25
30

Figure 3a

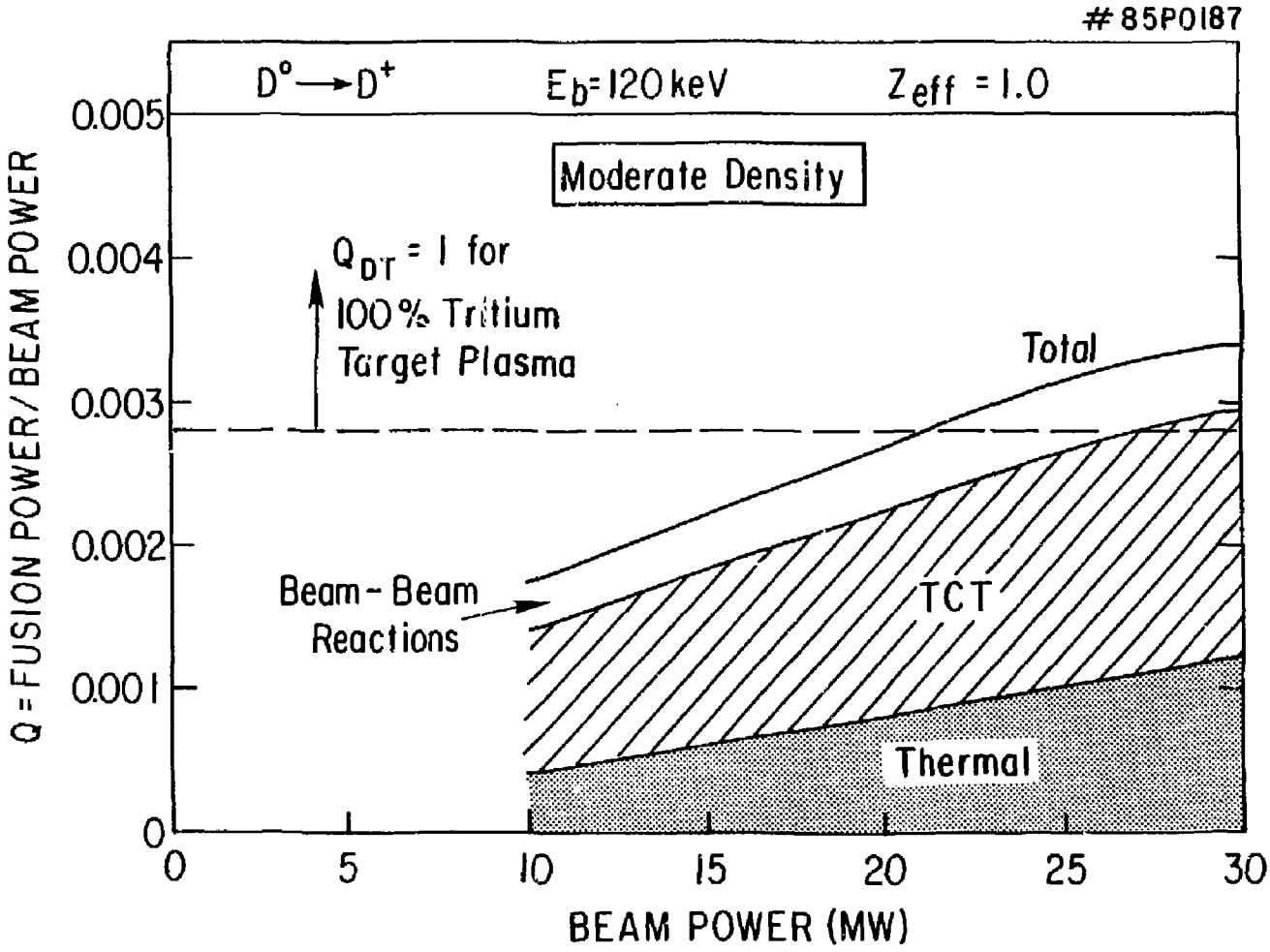
#85P0187
D° → D+
Eb=120 keV
Zeff = 1.0
Moderate Density
QDT = 1 for
100% Tritium
Target Plasma
Total
Beam-Beam
Reactions
TCT
Thermal
Q = FUSION POWER/BEAM POWER
0.005
0.004
0.003
0.002
0.001
0
0
5
10
15
20
25
30
BEAM POWER (MW)

Figure 3b

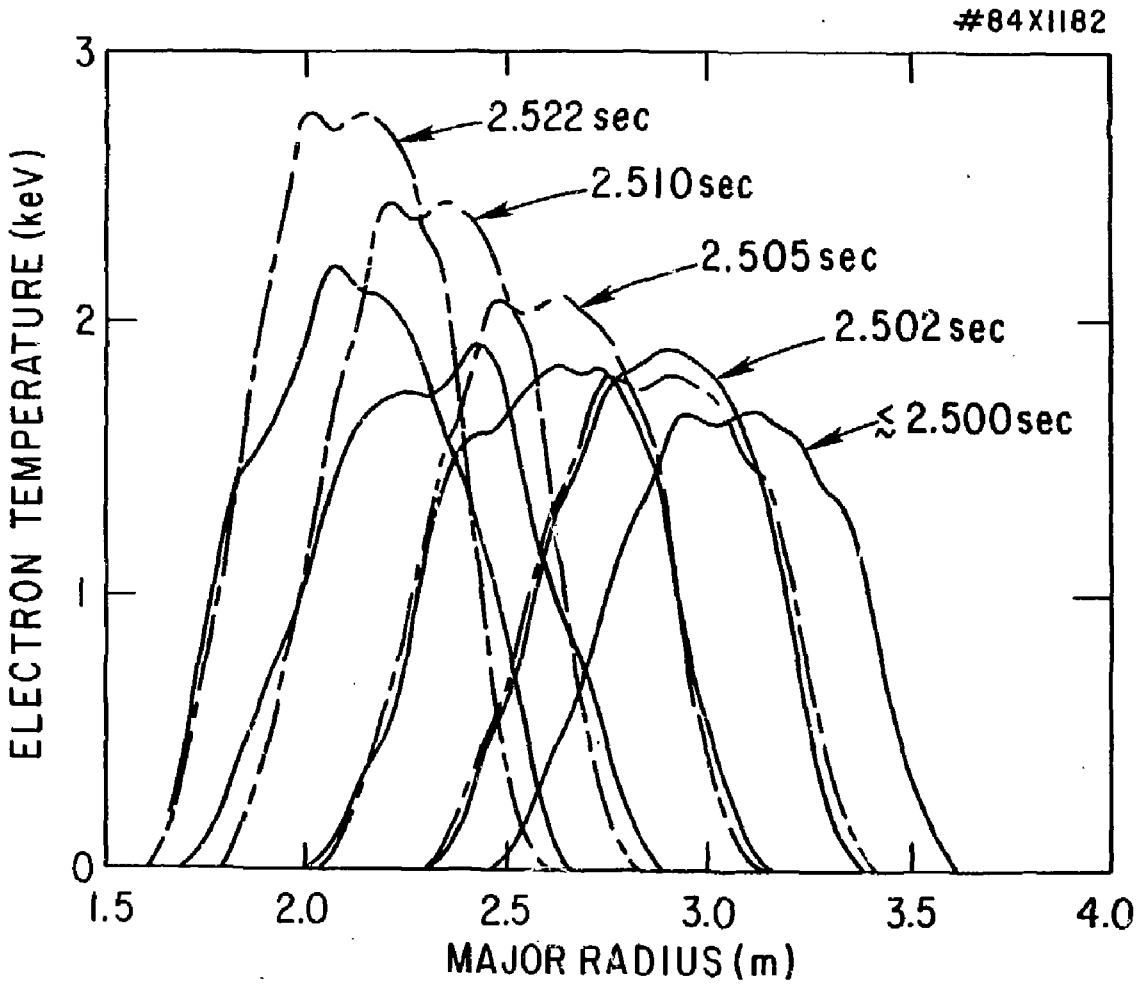
#84X1182
2.522 sec
2.510 sec
2.505 sec
2.502 sec
≲ 2.500 sec
ELECTRON TEMPERATURE (keV)
MAJOR RADIUS (m)
0
1
2
3
1.5
2.0
2.5
3.0
3.5
4.0

Figure 4

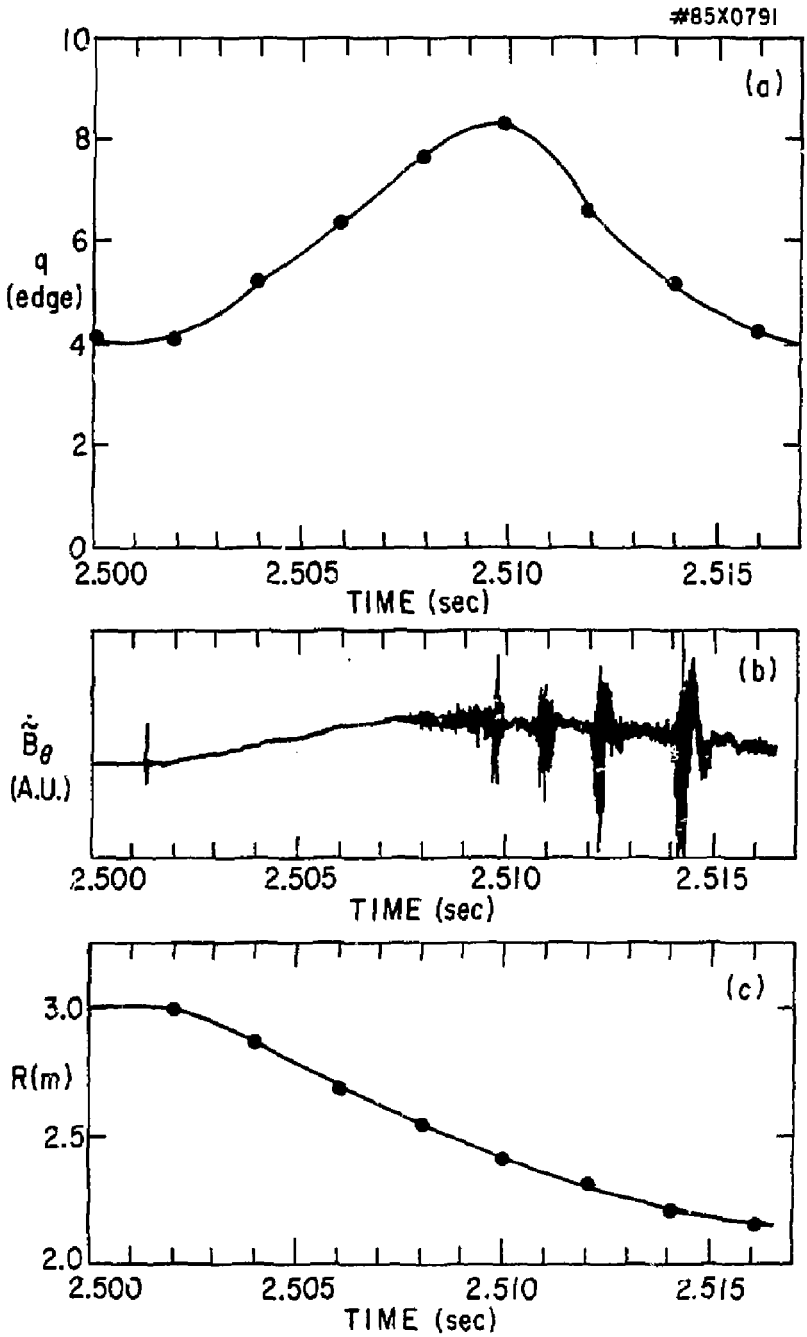
#85X0791
(a)
q
(edge)
10
8
6
4
2
0
2.500
2.505
2.510
2.515
TIME (sec)
(b)
$\tilde{B}_\theta$
(A.U.)
2.500
2.505
2.510
2.515
TIME (sec)
(c)
R(m)
3.0
2.5
2.0
2.500
2.505
2.510
2.515
TIME (sec)

Figure 5

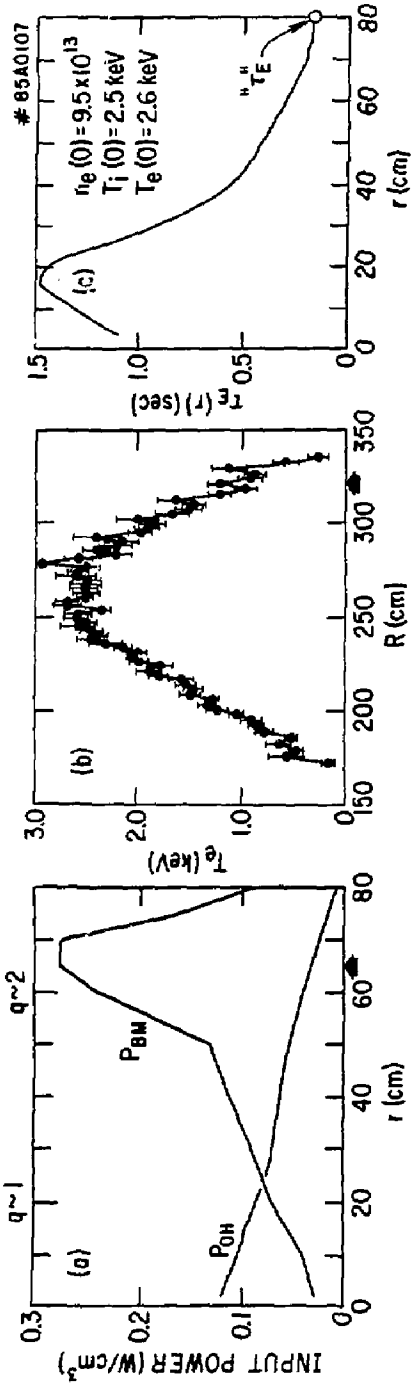
INPUT POWER (W/cm³)
0.3
0.2
0.1
0
q~1
q~2
(a)
P_OH
P_BM
0
20
40
60
80
r (cm)
T_e (keV)
3.0
2.0
1.0
0
(b)
150
200
250
300
350
R (cm)
τ_E (r) (sec)
1.5
1.0
0.5
0
(c)
85A0107
n_e(0) = 9.5x10^13
T_i(0) = 2.5 keV
T_e(0) = 2.6 keV
τ_E^H
0
20
40
60
80
r (cm)

Figure 6

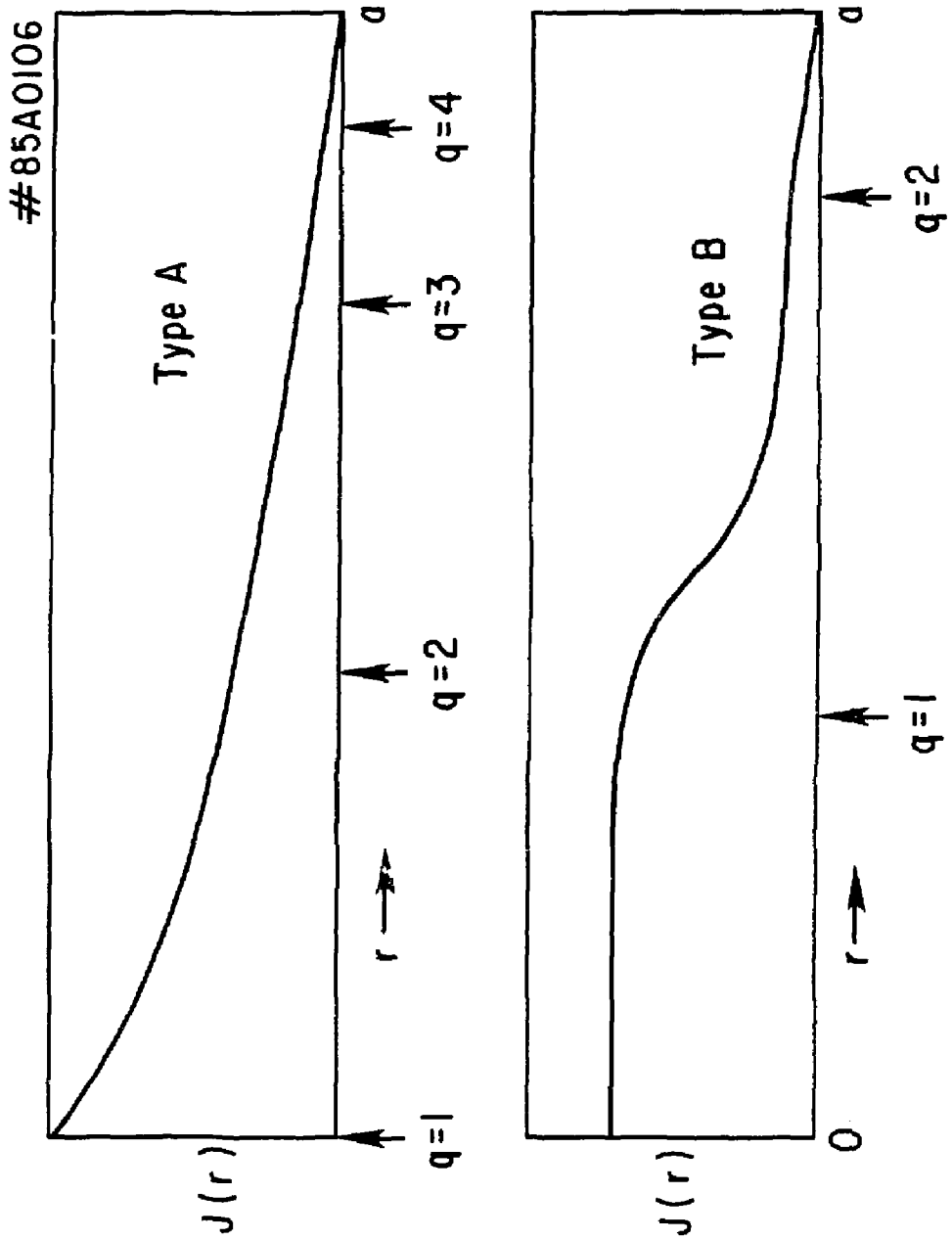

Figure 7

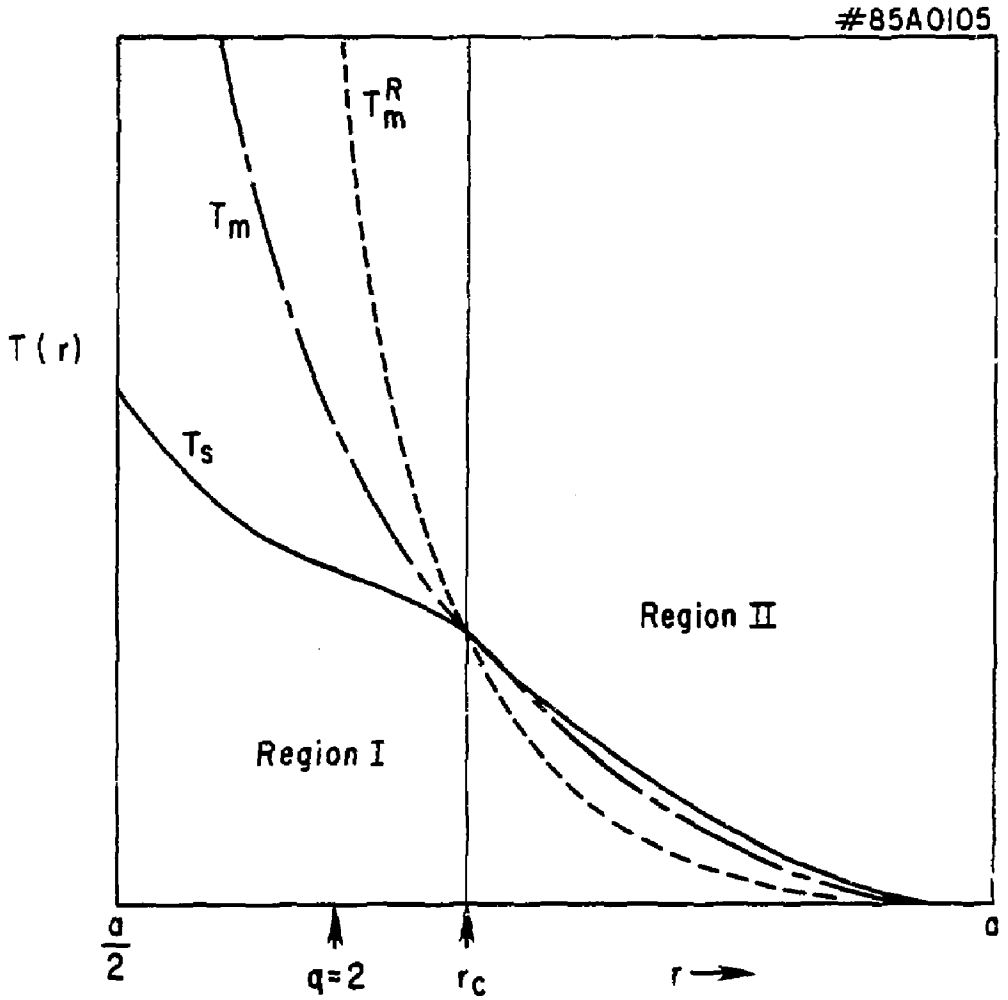

Figure 8

EXTERNAL DISTRIBUTION IN ADDITION TO UC-20

Plasma Res Lab, Austra Nat'l Univ, AUSTRALIA
Dr. Frank J. Paoloni, Univ of Wollongong, AUSTRALIA
Prof. I.R. Jones, Flinders Univ., AUSTRALIA
Prof. M.H. Brennan, Univ Sydney, AUSTRALIA
Prof. F. Cap, Inst Theo Phys, AUSTRIA
Prof. Frank Verheest, Inst theoretische, BELGIUM
Dr. D. Palumbo, Dg XII Fusion Prog, BELGIUM
Ecole Royale Militaire, Lab de Phys Plasmas, BELGIUM
Dr. P.H. Sakanaka, Univ Estadual, BRAZIL
Dr. C.R. James, Univ of Alberta, CANADA
Prof. J. Teichmann, Univ of Montreal, CANADA
Dr. H.M. Skarsgard, Univ of Saskatchewan, CANADA
Prof. S.R. Sreenivasan, University of Calgary, CANADA
Prof. Tudor W. Johnston, INRS-Energie, CANADA
Dr. Hannes Barnard, Univ British Columbia, CANADA
Dr. M.P. Bachynski, MPB Technologies, Inc., CANADA
Chalk River, Nucl Lab, CANADA
Zhengwu Li, SW Inst Physics, CHINA
Library, Tsing Hua University, CHINA
Librarian, Institute of Physics, CHINA
Inst Plasma Phys, Academia Sinica, CHINA
Dr. Peter Lukac, Komenskeho Univ, CZECHOSLOVAKIA
The Librarian, Culham Laboratory, ENGLAND
Prof. Schatzman, Observatoire de Nice, FRANCE
J. Radet, CEN-BP6, FRANCE
AM Dupas Library, AM Dupas Library, FRANCE
Dr. Tom Mual, Academy Bibliographic, HONG KONG
Preprint Library, Cent Res Inst Phys, HUNGARY
Dr. R.K. Chhajlani, Vikram Univ. INDIA
Dr. B. Dasgupta, Saha Inst, INDIA
Dr. P. Kaw, Physical Research Lab, INDIA
Dr. Phillip Rosenau, Israel Inst Tech, ISRAEL
Prof. S. Cuperman, Tel Aviv University, ISRAEL
Prof. G. Rostagni, Univ Di Padova, ITALY
Librarian, Int'l Ctr Theo Phys, ITALY
Miss Clelia De Palo, Assoc EURATOM-ENEA, ITALY
Biblioteca, del CNR EURATOM, ITALY
Dr. H. Yamato, Toshiba Res & Dev, JAPAN
Direc. Dept. Lg. Tokamak Dev. JAERI, JAPAN
Prof. Nobuyuki Inoue, University of Tokyo, JAPAN
Research Info Center, Nagoya University, JAPAN
Prof. Kyoji Nishikawa, Univ of Hiroshima, JAPAN
Prof. Sigeru Mori, JAERI, JAPAN
Prof. S. Tanaka, Kyoto University, JAPAN
Library, Kyoto University, JAPAN
Prof. Ichiro Kawakami, Nihon Univ, JAPAN
Prof. Satoshi Itoh, Kyushu University, JAPAN
Dr. D.I. Choi, Adv. Inst Sci & Tech, KOREA
Tech Info Division, KAERI, KOREA
Bibliotheek, Fom-Inst Voor Plasma, NETHERLANDS
Prof. B.S. Liley, University of Waikato, NEW ZEALAND
Prof. J.A.C. Cabral, Inst Superior Tecn, PORTUGAL
Dr. Octavian Petrus, ALI CUZA University, ROMANIA
Prof. M.A. Hellberg, University of Natal, SO AFRICA
Dr. Johan de Villiers, Plasma Physics, Nucor, SO AFRICA
Fusion Div. Library, JEN, SPAIN
Prof. Hans Wilhelmson, Chalmers Univ Tech, SWEDEN
Dr. Lennart Stenflo, University of UMEA, SWEDEN
Library, Royal Inst Tech, SWEDEN
Centre de Recherchesen, Ecole Polytech Fed, SWITZERLAND
Dr. V.T. Tolok, Kharkov Phys Tech Ins, USSR
Dr. D.D. Ryutov, Siberian Acad Sci, USSR
Dr. G.A. Eliseev, Kurchatov Institute, USSR
Dr. V.A. Glukhikh, Inst Electro-Physical, USSR
Institute Gen. Physics, USSR
Prof. T.J.M. Boyd, Univ College N Wales, WALES
Dr. K. Schindler, Ruhr Universitat, W. GERMANY
Nuclear Res Estab, Julich Ltd, W. GERMANY
Librarian, Max-Planck Institut, W. GERMANY
Bibliothek, Inst Plasmaforschung, W. GERMANY
Prof. R.K. Janev, Inst Phys, YUGOSLAVIA